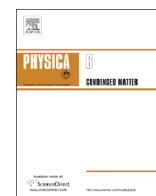




ELSEVIER

Contents lists available at ScienceDirect

Physica B

journal homepage: [www.elsevier.com/locate/physb](http://www.elsevier.com/locate/physb)

# Scaling of dynamical decoupling for a single electron spin in nanodiamonds at room temperature

Dong-Qi Liu, Gang-Qin Liu, Yan-Chun Chang, Xin-Yu Pan\*

Beijing National Laboratory for Condensed Matter Physics, Institute of Physics, Chinese Academy of Sciences, Beijing 100190, China

## ARTICLE INFO

### Article history:

Received 27 November 2012

Received in revised form

16 September 2013

Accepted 18 September 2013

Available online 25 September 2013

### Keywords:

Nanodiamond

Nitrogen-vacancy center

Dynamical decoupling

Spin bath

Noise spectrum

## ABSTRACT

Overcoming the spin qubit decoherence is a challenge for quantum science and technology. We investigate the decoherence process in nanodiamonds by Carr–Purcell–Meiboom–Gill (CPMG) technique at room temperature. We find that the coherence time  $T_2$  scales as  $n^\gamma$ . The elongation effect of coherence time can be represented by a constant power of the number of pulses  $n$ . Considering the filter function of CPMG decoupling sequence as a  $\delta$  function, the spectrum density of noise has been reconstructed directly from the coherence time measurements and a Lorentzian noise power spectrum model agrees well with the experiment. These results are helpful for the application of nanodiamonds to nanoscale magnetic imaging.

© 2013 Elsevier B.V. All rights reserved.

## 1. Introduction

The nitrogen-vacancy (NV) center in diamond has drawn much attention because of its long coherence time at room temperature and controllable hyperfine interaction with surrounding nuclear spins [1–5]. The long coherence time of NV center electron spin is important for applying it in quantum information processing (QIP) or nanoscale magnetometry [6,7]. Dynamical decoupling technique consists of a sequence of control pulses and can effectively suppress the environment noise [8,9]. Typically in a high-purity diamond sample (type IIa) the decoherence process of center electron spin is affected by the  $^{13}\text{C}$  spin bath. Ryan and co-authors used dynamical decoupling technique to extend the coherence of NV spin from 220  $\mu\text{s}$  to an effective  $T_2$  over 1.6 ms [10]. In high nitrogen concentration diamond (type Ib), the bath is mainly composed of electron spins localized on nitrogen impurity atoms. In a type Ib diamond sample de Lange and co-authors demonstrated a strong suppression of the coupling of a single spin in diamond with the surrounding spin bath by using double-axis dynamical decoupling [11].

Comparing with bulk diamond, nanodiamond plays an important role in many applications such as biological imaging [12], plasmon-enhanced single photon emission [13] and nanoscale imaging magnetometry [14,15]. In a nanodiamond, however, the spin environment is very complicated. It is mainly composed of

nitrogen impurities, lattice imperfections and surface spins due to dangling bonds. These paramagnetic center spins always make NV spin dephase. The dephasing time of NV spin in nanodiamonds is always short, typically from several hundred of nanoseconds to some microseconds [16]. Dynamical decoupling technology can prolong the coherence time of NV center in nanodiamond. Naydenov and co-authors have conducted a preliminary investigation on coherence enhancement of NV spin in nanodiamonds through CPMG technology [17]. In this paper, we also obtain the coherence enhancement, and then find a power-law scaling relationship between the coherence time  $T_2$  and the number of pulses  $n$ :  $T_2 \propto n^\gamma$ , with  $\gamma$  independent of the envelope function used to extract  $T_2$ . Furthermore, considering that the NV center can be taken as a probe to investigate the dynamics of spin environment through the interaction between NV and paramagnetic centers, the dynamical decoupling results provide important information about the spectral form of the spin environment noise.

## 2. Experiment

An NV center comprises a substitutional nitrogen atom instead of a carbon atom and an adjacent lattice vacancy. The negatively charged NV center is  $S=1$  and is the one studied here. The electronic paramagnetic ground state of NV center is a spin triplet state ( $^3\text{A}$ ,  $S=1$ ). As a result of crystal field [18,19], there is a zero field splitting  $D=2.87$  GHz between sublevels of  $m_s=0$  and  $m_s=\pm 1$  ( $m_s$  is the projection of spin operator along the  $z$ -axis).

\* Corresponding author. Tel.: +86 10 82649211; fax: +86 10 82640266.  
E-mail address: [xypan@aphy.iphy.ac.cn](mailto:xypan@aphy.iphy.ac.cn) (X.-Y. Pan).

Due to  $C_{3v}$  symmetry,  $m_s = +1$  and  $m_s = -1$  levels are degenerated at zero magnetic field. While an applied magnetic field lifts the  $m_s = +1$  and  $m_s = -1$  degeneracy. In the presence of optical excitation, NV spin is polarized into  $m_s = 0$  sublevel [20]. Average photon emission rate for transitions involving the level  $m_s = 0$  is quite bigger than that for transitions involving the levels  $m_s = \pm 1$ , which allows readout of the spin state by spin-selective fluorescence [21]. Different non-radiative decay pathways for the  $m_s = 0$  and  $m_s = \pm 1$  spin projections from the triplet excited state  ${}^3E$  to the triplet ground state  ${}^3A_2$  via intermediate dark states (singlet states,  ${}^1A_1$  and  ${}^1E$ ) are assumed to be responsible for these phenomena [22–24].

Our samples are commercial diamond nanocrystals (10–100 nm, Element Six). They were irradiated by 6 MeV electrons at a dose of  $4.8 \times 10^{15}$  electrons  $\text{cm}^{-2}$  and subsequently annealed at 800 °C for 2 h under vacuum to create NV centers. The annealed samples were then oxidized at 550 °C for 1 h to purify the nanodiamond surface. The remained samples were suspended in deionized water and ultrasonicated about 1 h, then centrifuged for 10 min at 5000 rpm. The supernatants were then spin-coated onto the glass substrate. The average distance between fluorescence nanodiamonds is about 3  $\mu\text{m}$ , which is bigger than the resolution ( $\sim 500$  nm) of our test system.

Single NV centers hosted in nanodiamonds were individually addressed by home built scanning confocal microscope system, as shown in Fig. 1a. A Hanbury Brown-Twiss setup is used to measure the fluorescence autocorrelation function  $g^2(\tau)$  and  $g^2(0) < 0.5$  indicates that it is a single NV center (data not shown). NV centers were excited by a 532 nm continuous laser through an objective (Olympus, numerical aperture=0.9). The fluorescence emitted by the NV was collected by the same objective, and then filtered by a 650 nm long-pass filter, then detected by a single photon counting module (Perkin-Elmer, SPCM). A static magnetic field (84 G) was

applied along the NV center symmetry axis to split the  $m_s = \pm 1$  sublevels (Fig. 1b). A difference between bulk diamond and nanodiamond is the orientation of symmetry axis of NV center. For a bulk diamond single-crystal, all NV center contained only have four possible orientations due to the  $C_{3v}$  symmetry of the NV center in the diamond lattice. However, irregularly shaped nanodiamonds are spin-coated on the substrate randomly. Therefore, the orientations of all single NV centers in nanodiamonds are random. The alignment of magnetic field applied along the symmetry axis of NV center in nanodiamond is achieved by measurement of continuous-wave optically detected magnetic resonance (CW ODMR) spectrum [25]. The CW ODMR spectrum for NV S1 is shown in Fig. 1b. We chose the  $m_s = 0 \leftrightarrow m_s = -1$  transition and the frequency 2.630 GHz is far away from the  $m_s = 0 \leftrightarrow m_s = +1$  transition frequency 3.102 GHz.

To promote the stability and intensity of microwave field, a coplanar waveguide (CPW) transmission line was fabricated. A photoresist was spin-coated on a clean silica glass. After baking, a prepared shadow mask was placed on the top of the photoresist film and exposed to the Ultraviolet light of mask aligner (MA6, Karl) about 15 s. Thus the mask patterns were printed on the photoresist film. Then the resist film with patterns was immersed into a developer for 40 s. After oxygen plasma etching, metal layers of 5 nm Pt and 100 nm Au were deposited on the substrate, respectively. After cooling down, followed by cleaning with acetone, the CPW transmission line with 20  $\mu\text{m}$  gaps was fabricated (Fig. 1a inset). A microwave source (Agilent, E4422B) was used to generate the microwave signal and the signal was amplified by a high power amplifier, then sent into the CPW for manipulation of NV center electron spin state. The Rabi frequency reached up to 50 MHz. The Rabi frequency used in experiment was about 16 MHz (Fig. 1c). In addition, pulse errors will affect the results

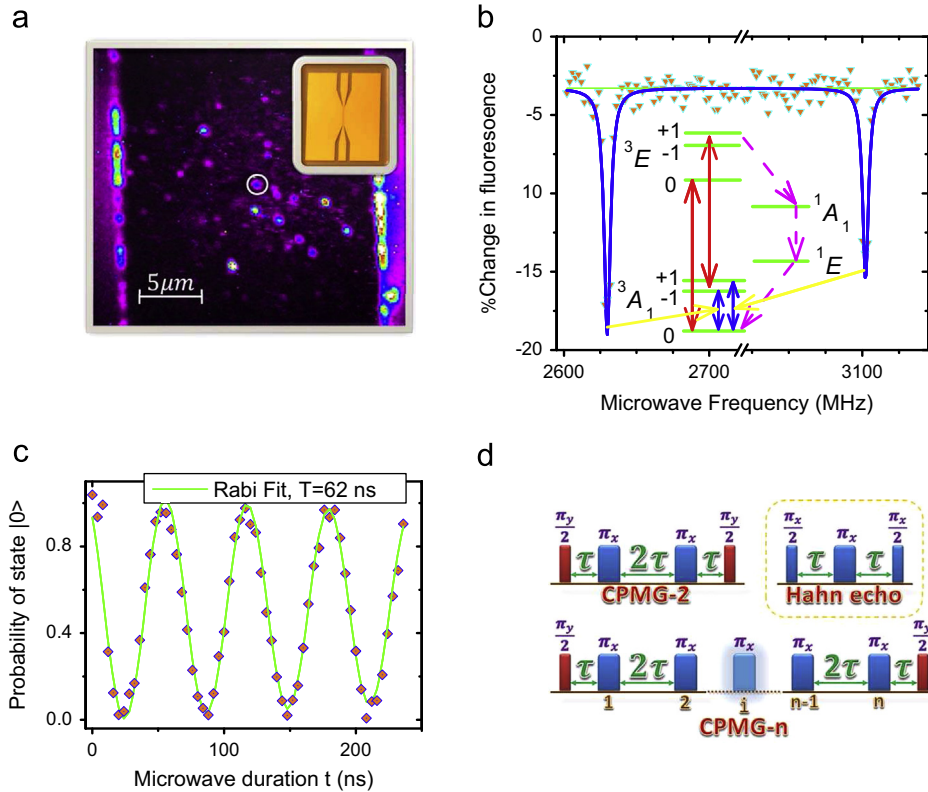


**Fig. 1.** Detection and manipulation of the qubit. (a) Fluorescence image of nanodiamond prepared on the CPW transmission line. NV S1 is circled. The inset is a photo of CPW with 20  $\mu\text{m}$  gaps fabricated on a silica glass. (b) CW ODMR spectrum for NV S1. The inset is energy levels of NV center. A 532 nm laser is used to excite and initialize the NV center. Fluorescence is collected by a confocal microscope. (c) Rabi oscillation of NV S1. Rabi oscillation period is about 62 ns. (d) Hahn echo and CPMG control pulse sequences.  $\pi_x$  ( $\pi_y$ ) implies the direction of microwave magnetic fields parallel to  $x$  ( $y$ ).

Download English Version:

<https://daneshyari.com/en/article/1810005>

Download Persian Version:

<https://daneshyari.com/article/1810005>

[Daneshyari.com](https://daneshyari.com)